Journal of Alloys and Compounds 516 (2012) 9–15

Contents lists available at SciVerse ScienceDirect

Journal of Alloys and Compounds

journal homepage: www.elsevier.com/locate/jallcom

The 620 °C and 800 °C isothermal sections of the Zn–Fe–Cu ternary system

Haoping Peng[a], Xuping Su[a,b,c,*], Zhi Li[a], Xiaoqin Li[a], Jianhua Wang[b,c], Ya Liu[b,c], Hao Tu[b,c]

[a] Key Laboratory of Materials Design and Preparation Technology of Hunan Province, Xiangtan University, 411105 Hunan, PR China
[b] Key Laboratory of Advanced Metal Materials of Changzhou City, Changzhou University, Changzhou, 213164 Jiangsu, PR China
[c] School of Materials Science and Engineering, Changzhou University, Changzhou, 213164 Jiangsu, PR China

ARTICLE INFO

Article history:
Received 26 July 2011
Received in revised form 1 November 2011
Accepted 3 November 2011
Available online 26 November 2011

Keywords:
Zn–Fe–Cu
Phase diagram
Intermetallics
Bath
Galvalume

ABSTRACT

The 620 °C and 800 °C isothermal sections of the Zn–Fe–Cu ternary system were constructed based on Wave Dispersive X-ray Spectrometry (WDS) and X-ray power diffraction analysis (XRD). Four three-phase regions have been identified in the Zn–Fe–Cu ternary system at 620 °C, and three three-phase regions have been confirmed in the 800 °C isothermal section. All of the Fe solubility in η-Zn, β and (Cu) at 620 °C are lower than the solubility at 800 °C. The γ and Γ phases form a continuous solid solution at 620 °C, which is designated as the γ/Γ phase. Binary phases δ_{Fe} and δ_{Cu} extend into the ternary system at 620 °C, the three-phase triangle of ($\gamma/\Gamma + \delta_{Fe} + \delta_{Cu}$) is small and narrow.

1. Introduction

Hot-dipping coating is applied to improve atmospheric corrosion resistance for steel [1]. The corrosion resistance of the galvalume coated steel (55%Al–Zn–Si, wt%), which was developed and applied by the Bethlehem Steel Corporation, is superior to a single coating (Zn, Al) and 5 wt% Al–Zn coating. In the absence of other elements in Al–Zn bath, there is a violent reaction between steel matrix and Al–Zn bath, which would bring an adverse influence to the performance of coating. The addition of Si in the Al–Zn hot-dipping bath can change the interfacial intermetallic compound from Fe–Al phase to Fe–Al–Si phase, to restrain the strong and rapid exothermic reaction between the steel matrix and A1–Zn bath, and prevent rapid growth of alloy layer [2–4].

The earlier study showed a small amount of Cu added to hot-dipping aluminum bath would reduce the coating thickness, and improve the fluidity of molten zinc [5], whereas higher Cu content may damage the corrosion resistance of the coating [6]. When Cu is added into the Al–Zn bath, and Fe is dissolved into the molten bath, the bath essentially becomes a Zn–Fe–Al–Cu quaternary system. The existence of Cu in the bath may play the same role as Si. However, it is devoid of theoretical studies and practical applications in this field, especially, the information concerning phase equilibrium in the Zn–Fe–Cu system is limited. Miettinen [7] investigated the Zn–Fe–Cu ternary system. Due to the lack of experimental data from iron-rich alloys, the validity of the present description is verified only for Cu–Zn-rich alloys. Avettand-Fènoël et al. proposed the 460 °C Zn-rich corner of the Zn–Fe–Cu ternary phase diagram [8]. Budurov [9] reported the 700 °C isothermal sections of the Zn–Fe–Cu ternary system, which shows the γ (Cu_5Zn_8) and Γ (Fe_3Zn_{10}) phases form a continuous solid solution. In this work, the 620 °C and 800 °C isothermal sections of the Zn–Fe–Cu ternary system will be determined experimentally by using combined techniques of Scanning Electron Microscopy–Energy Dispersive X-ray spectrometry (SEM–EDS), Wave Dispersive X-ray spectrometry (WDS) and X-ray Diffraction (XRD). The experimental results will facilitate the explanation for the function of Cu in Al–Zn bath.

2. Binary systems

In terms of the current knowledge of phase equilibrium concerning the Zn–Fe, Zn–Cu and Fe–Cu binary systems, the following information should be mentioned. Due to its importance to the galvanizing industry, the Zn–Fe binary system has been studied by various authors [10–13]. There are two intermetallic compounds: Γ (Fe_3Zn_{10}), and δ_{Fe} ($FeZn_{10}$) at 620 °C. No intermetallic compound exists in the Zn–Fe system at 800 °C. The temperature of the Liq. + α-Fe ↔ Γ peritectic reaction is 782 °C, and the peritectic reaction Γ + Liq. ↔ δ_{Fe} occurs at 672 °C.

The Zn–Cu system was also assessed repeatedly [14–16], which contains three intermediate phases at 620 °C, namely β (CuZn), γ (Cu_5Zn_8) and δ_{Cu} ($CuZn_3$). The β and γ phases are stable below

* Corresponding author at: School of Materials Science and Engineering, Changzhou University, Changzhou, 213164 Jiangsu, PR China
Tel.: +86 519 86330982; fax: +86 519 86330171.
E-mail address: sxping@cczu.edu.cn (X. Su).

0925-8388/$ – see front matter © 2011 Elsevier B.V. All rights reserved.
doi:10.1016/j.jallcom.2011.11.018

Table 1
The crystallographic parameters of the binary compounds of the Zn–Fe and Zn–Cu systems.

Compound	Crystal system	Space group	Lattice parameters (nm)			Ref.
			a	*b*	*c*	
$\Gamma(Fe_3Zn_{10})$	Cubic body-centered	$I\bar{4}3m$(2 1 7)	0.898	–	–	[22]
$\delta_{Fe}(FeZn_{10})$	Hexagonal primitive	$P6_3mc$(1 8 6)	1.283	–	5.772	[22]
$\beta'(CuZn)$	Cubic primitive	$Pm\bar{3}m$(2 2 1)	0.2950	–	–	[23]
$\beta(CuZn)$	Cubic body-centered	$Im\bar{3}m$(2 2 9)	0.2945	–	–	[24]
$\gamma(Cu_5Zn_8)$	Cubic body-centered	$I\bar{4}3m$(2 1 7)	0.8866	–	–	[25]
$\delta_{Cu}(CuZn_3)$	Hexagonal primitive	$P\bar{6}$(1 7 4)	0.4275	–	0.259	[26]

834 °C. The reaction temperatures of order–disorder transformation of the β′–β are 454 °C (44.8 at.% Zn) and 468 °C (48.2 at.% Zn) respectively, in this system, and the γ + Liq. ↔ δ_{Cu} peritectic reaction occurs at 700 °C. Besides, the Fe–Cu binary system has been researched repetitiously [17–21]. No intermetallics exist in the Fe–Cu system. The solubility of Fe in (Cu) and Cu in α-Fe is less than 2.0 at.% below 900 °C. Crystallographic data of binary compounds mentioned above are shown in Table 1.

3. Experimental methods

The phase relationships of the Zn–Fe–Cu ternary system were deduced by studying the alloy samples, which were prepared using Zn block, Fe powder and Cu powder. The purities of the materials were 99.99 wt% and the powders used were −200 mesh size. The raw materials weighted 5 g in each alloy were mixed and sealed in an evacuated quartz tube. The mixture was heated to 1200 °C and kept for 24 h, then quenched in water with bottom-quenching technique [27], in order to obtain a relatively compact sample. The tube was turned upside down for several times during the melting process to thoroughly ensure homogeneity of the samples. The quenched samples were resealed individually in evacuated quartz tubes and annealed at 620 °C for 25 days and 820 °C for 15 days, respectively. At the end of the treatment, the samples were quenched rapidly into water to preserve the equilibrium state.

The specimens were prepared using conventional metallographic techniques, etched with aqueous solution mixed ferric chloride and hydrochloride (5 g $FeCl_3$, 50 ml HCl, 100 ml H_2O) for microstructure examination. The morphology and chemical composition analyses of phases in the alloys were performed in a JSM-6510 Scanning Electron Microscopy equipped with OXFORD Energy Dispersive X-ray Spectrometer and Wave Dispersive X-ray Spectrometer. The operating voltage of the SEM was 20 kV. The phase constitutions of the alloys were further confirmed by analyzing X-ray Powder Diffraction patterns, which are generated by X-ray diffractometer with Cu K_α radiation.

4. Results and discussion

A series of alloys were prepared for studying phase relationships of the Zn–Fe–Cu ternary system at 620 °C and 800 °C. Their design compositions are listed in Table 2. These compositions were selected in the surrounding regions of binary compounds listed in Table 1, convenient for studying their phase relationships. Phases in alloys can be easily differentiated based on the relief, color and chemical composition. In general, the different relief is distinguishable on the SEM micrographs, and chemical compositions can be analyzed using the SEM–WDS technique. Meanwhile, the phases can be confirmed in further by analyzing their X-ray diffraction patterns. The 620 °C and 800 °C isothermal sections of the Zn–Fe–Cu system with the indication of the compositions of the designed alloys (•) are shown in Figs. 1 and 2, respectively.

4.1. The 620 °C isothermal sections of the Zn–Fe–Cu ternary system

For studying the 620 °C isothermal section of the Zn–Fe–Cu ternary system, all phase found in twenty-two primary alloys are summarized in Table 3. Alloy A1–A4 were prepared to determine phase relationships in the Zn-rich corner at 620 °C. The microstructure of alloy A2 is given in Fig. 3a, which indicates that alloy 2 consists of three phases. SEM–WDS analyses suggested that they are η-Zn, δ_{Fe} and δ_{Cu}. The δ_{Fe} and δ_{Cu} phases exist in the matrix of the η-Zn phase. The equilibrium relationship of η-Zn, δ_{Fe} and δ_{Cu} in alloy A2 has been confirmed once again by X-ray diffraction pattern (Fig. 3b). It needs to pay attention that the η-Zn phase which was in liquid state at the test temperature, it transformed into solid

Table 2
Nominal composition of ternary alloys (at.%).

Alloy	Design composition	Phase present	
		620 °C	800 °C
A1	Zn_{94}–Fe_2–Cu_4	η-Zn + δ_{Fe}	–
A2	Zn_{85}–Fe_2–Cu_{13}	η-Zn + δ_{Fe} + δ_{Cu}	η-Zn
A3	Zn_{79}–Fe_2–Cu_{19}	η-Zn + δ_{Cu}	η-Zn
A4	Zn_{78}–Fe_4–Cu_{18}	δ_{Fe} + δ_{Cu}	–
A5	Zn_{76}–Fe_6–Cu_{18}	γ/Γ + δ_{Fe} + δ_{Cu}	–
A6	Zn_{80}–Fe_{10}–Cu_{10}	γ/Γ + δ_{Fe}	α-Fe + η-Zn
A7	Zn_{75}–Fe_{10}–Cu_{15}	γ/Γ	α-Fe + η-Zn
A8	Zn_{71}–Fe_{10}–Cu_{19}	γ/Γ	α-Fe + η-Zn + γ
A9	Zn_{69}–Fe_{10}–Cu_{21}	γ/Γ	α-Fe + η-Zn + γ
A10	Zn_{66}–Fe_2–Cu_{32}	γ/Γ	γ
A11	Zn_{60}–Fe_{10}–Cu_{30}	α-Fe + γ/Γ	α-Fe + γ
A12	Zn_{62}–Fe_{10}–Cu_{28}	α-Fe + γ/Γ	α-Fe + γ
A13	Zn_{65}–Fe_{10}–Cu_{25}	α-Fe + γ/Γ	–
A14	Zn_{64}–Fe_{18}–Cu_{18}	α-Fe + γ/Γ	–
A15	Zn_{64}–Fe_{22}–Cu_{14}	α-Fe + γ/Γ	–
A16	Zn_{64}–Fe_{24}–Cu_{12}	α-Fe + γ/Γ	–
A17	Zn_{64}–Fe_{28}–Cu_8	α-Fe + γ/Γ	–
A18	Zn_{64}–Fe_{30}–Cu_6	α-Fe + γ/Γ	–
A19	Zn_{50}–Fe_{10}–Cu_{40}	α-Fe + γ + β	α-Fe + γ + β
A20	Zn_{40}–Fe_{10}–Cu_{50}	α-Fe + β	α-Fe + β
A21	Zn_{33}–Fe_{10}–Cu_{57}	α-Fe + β + (Cu)	α-Fe + β + (Cu)
A22	Zn_{20}–Fe_{10}–Cu_{70}	α-Fe + (Cu)	α-Fe + (Cu)

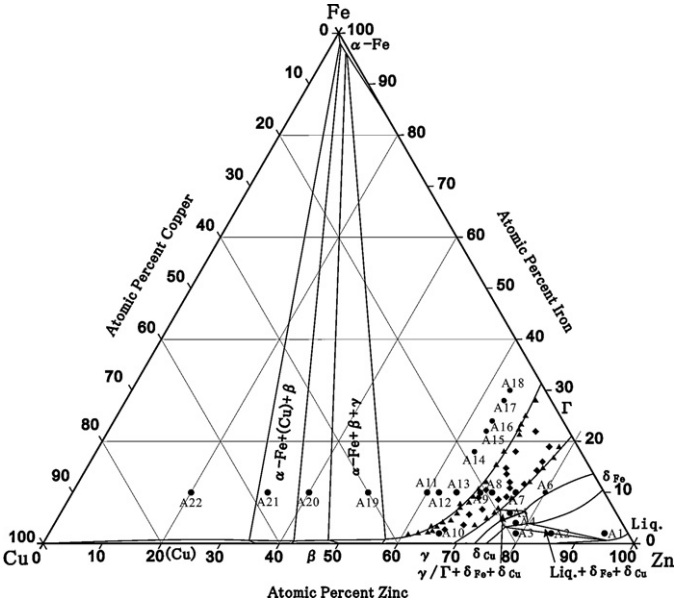

Fig. 1. The 620 °C isothermal section of the Zn–Fe–Cu ternary system. (•) Alloy compositions studied in this work; (♦) alloys situated within the γ (or Γ) phase; (▲) he compositions of γ (or Γ) phase boundary.

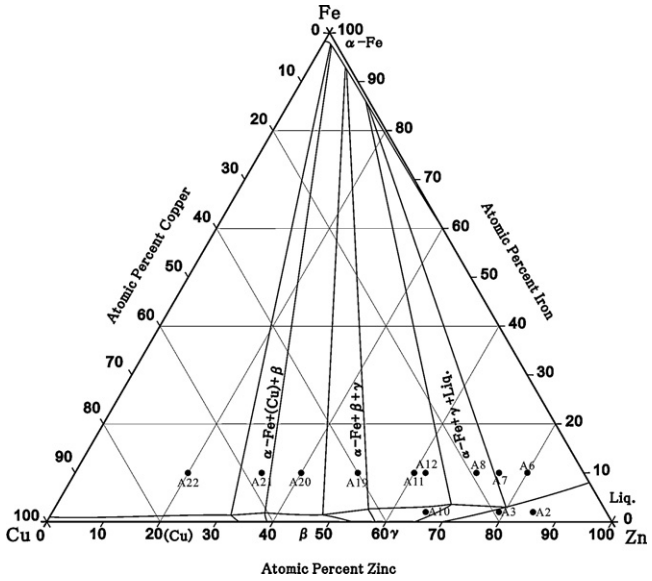

Fig. 2. The 800 °C isothermal section of the Zn–Fe–Cu ternary system. The signs in the diagram stand for the alloy compositions studied in this work.

Table 3
Specimens and phase compositions in the Zn–Fe–Cu ternary system at 620 °C.

Alloy	Designed composition	Phase	Composition (at.%)		
			Zn	Fe	Cu
A1	Zn_{94}–Fe_2–Cu_4	η-Zn	96.3	0.9	2.8
		δ_{Fe}	86.0	5.9	8.1
A2	Zn_{85}–Fe_2–Cu_{13}	η-Zn	94.8	0.5	4.7
		δ_{Fe}	80.2	3.9	15.9
		δ_{Cu}	76.7	3.2	20.1
A3	Zn_{79}–Fe_2–Cu_{19}	η-Zn	92.8	0.3	6.9
		δ_{Cu}	76.1	2.2	21.7
A4	Zn_{78}–Fe_4–Cu_{18}	δ_{Fe}	79.6	4.6	15.8
		δ_{Cu}	75.3	3.5	21.2
A5	Zn_{76}–Fe_6–Cu_{18}	γ/Γ	74.2	6.5	19.3
		δ_{Fe}	78.6	6.2	15.2
		δ_{Cu}	75.4	4.3	20.3
A6	Zn_{80}–Fe_{10}–Cu_{10}	δ_{Fe}	80.2	9.5	10.3
		γ/Γ	76.2	12.1	11.7
A7	Zn_{75}–Fe_{10}–Cu_{15}	γ/Γ	73.4	11.2	15.4
A8	Zn_{71}–Fe_{10}–Cu_{19}	γ/Γ	69.8	10.4	19.8
A9	Zn_{69}–Fe_{10}–Cu_{21}	γ/Γ	68.7	10.2	21.1
A10	Zn_{66}–Fe_2–Cu_{32}	γ/Γ	64.7	2.5	32.8
A11	Zn_{60}–Fe_{10}–Cu_{30}	α-Fe	6.2	93.2	0.6
		γ/Γ	63.9	3.2	32.9
A12	Zn_{62}–Fe_{10}–Cu_{28}	α-Fe	7.4	92.1	0.5
		γ/Γ	67.4	4.2	28.4
A13	Zn_{65}–Fe_{10}–Cu_{25}	α-Fe	8.4	91.2	0.4
		γ/Γ	66.8	7.6	25.6
A14	Zn_{64}–Fe_{18}–Cu_{18}	α-Fe	9.9	89.7	0.4
		γ/Γ	71.8	8.1	20.1
A15	Zn_{64}–Fe_{22}–Cu_{14}	α-Fe	11.2	88.5	0.3
		γ/Γ	72.0	12.2	15.9
A16	Zn_{64}–Fe_{24}–Cu_{12}	α-Fe	11.8	87.9	0.3
		γ/Γ	67.3	18.9	13.8
A17	Zn_{64}–Fe_{28}–Cu_8	α-Fe	12.9	86.9	0.2
		γ/Γ	66.4	23.5	10.2
A18	Zn_{64}–Fe_{30}–Cu_6	α-Fe	13.5	86.3	0.2
		γ/Γ	68.5	23.5	8.1
A19	Zn_{50}–Fe_{10}–Cu_{40}	α-Fe	3.3	95.9	0.8
		γ	57.5	0.8	41.7
		β	47.9	0.6	51.5
A20	Zn_{40}–Fe_{10}–Cu_{50}	α-Fe	2.3	96.9	0.8
		β	44.2	0.6	55.2
A21	Zn_{33}–Fe_{10}–Cu_{57}	α-Fe	1.4	97.7	0.9
		β	42.2	0.5	57.3
		(Cu)	34.7	0.6	64.7
A22	Zn_{20}–Fe_{10}–Cu_{70}	α-Fe	0.7	98.8	0.5
		(Cu)	21.4	0.8	77.8

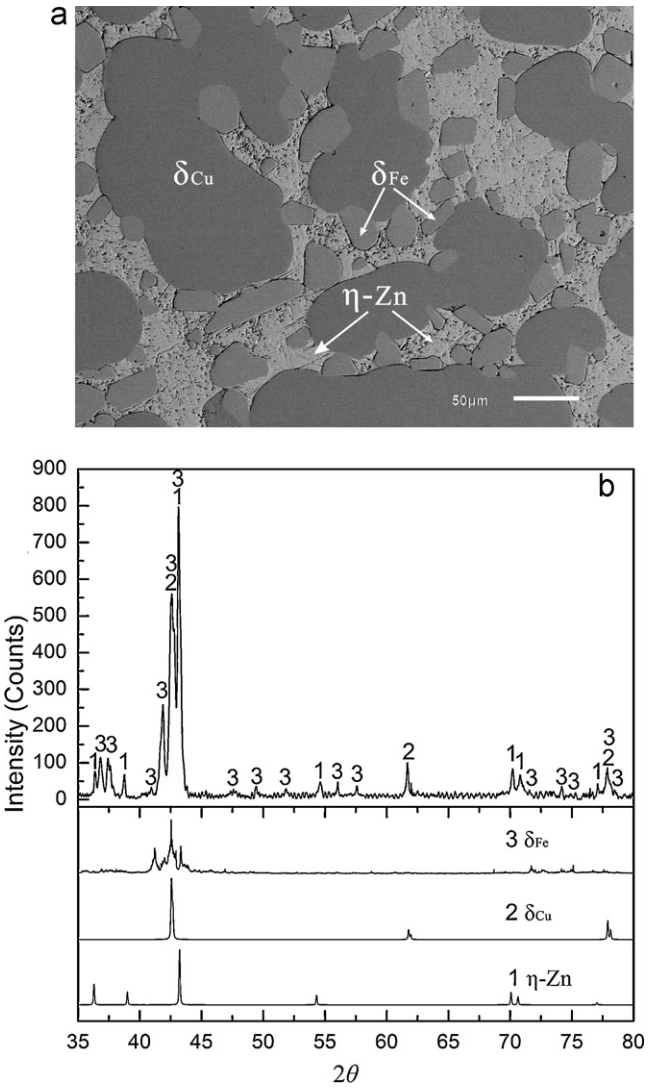

Fig. 3. The BSE micrograph of alloy A2 (Zn_{85}–Fe_2–Cu_{13}) at 620 °C indicates that it consists of three phases: η-Zn, δ_{Fe} and δ_{Cu}. (b) X-ray diffraction pattern of alloy A2 (Zn_{85}–Fe_2–Cu_{13}) confirms there are η-Zn, δ_{Fe} and δ_{Cu} in alloy A2 at 620 °C.

during quenching. WDS analyses indicated that the δ_{Fe} phase contains 80.2 at.% Zn, 3.9 at.% Fe and 15.9 at.% Cu. The solubility of Cu in the δ_{Fe} phase is higher than the result obtained by Avettand-Fènoël et al. [8] at 460 °C. The δ_{Cu} phase contains 76.7 at.% Zn, 3.2 at.% Fe and 20.1 at.% Cu. The existences of the three two-phase regions, η-Zn + δ_{Fe} (alloy A1), η-Zn + δ_{Cu} (alloy A3) and δ_{Fe} + δ_{Cu} (alloy A4), also confirms that the three-phase region (η-Zn + δ_{Fe} + δ_{Cu}) exists in 620 °C isothermal section.

The compositions of alloy A5–A18 were designed in regions near the γ phase and the Γ phase at 620 °C. The microstructure analyses of alloy A11–A18 showed that all of them comprise two phases which consist of α-Fe and γ (or Γ). Backscattered Electron (BSE) micrograph and phase composition analyses revealed that the two-phase equilibrium relationship of γ and Γ is undetected in alloy A11–A18. A typical microstructure is shown in Fig. 4a. SEM–WDS analyses indicated that there are α-Fe and γ in alloy A11, and the α-Fe phase contains 6.2 at.% Zn, 93.2 at.% Fe and 0.6 at.% Cu, while the γ phase contains 63.9 at.% Zn, 3.2 at.% Fe and 32.9 at.% Cu. X-ray diffraction studies confirmed that these phases are indeed α-Fe and γ.

Additional alloys were also designed to study the phase relationship of the γ and Γ phases. The compositions of the γ phase

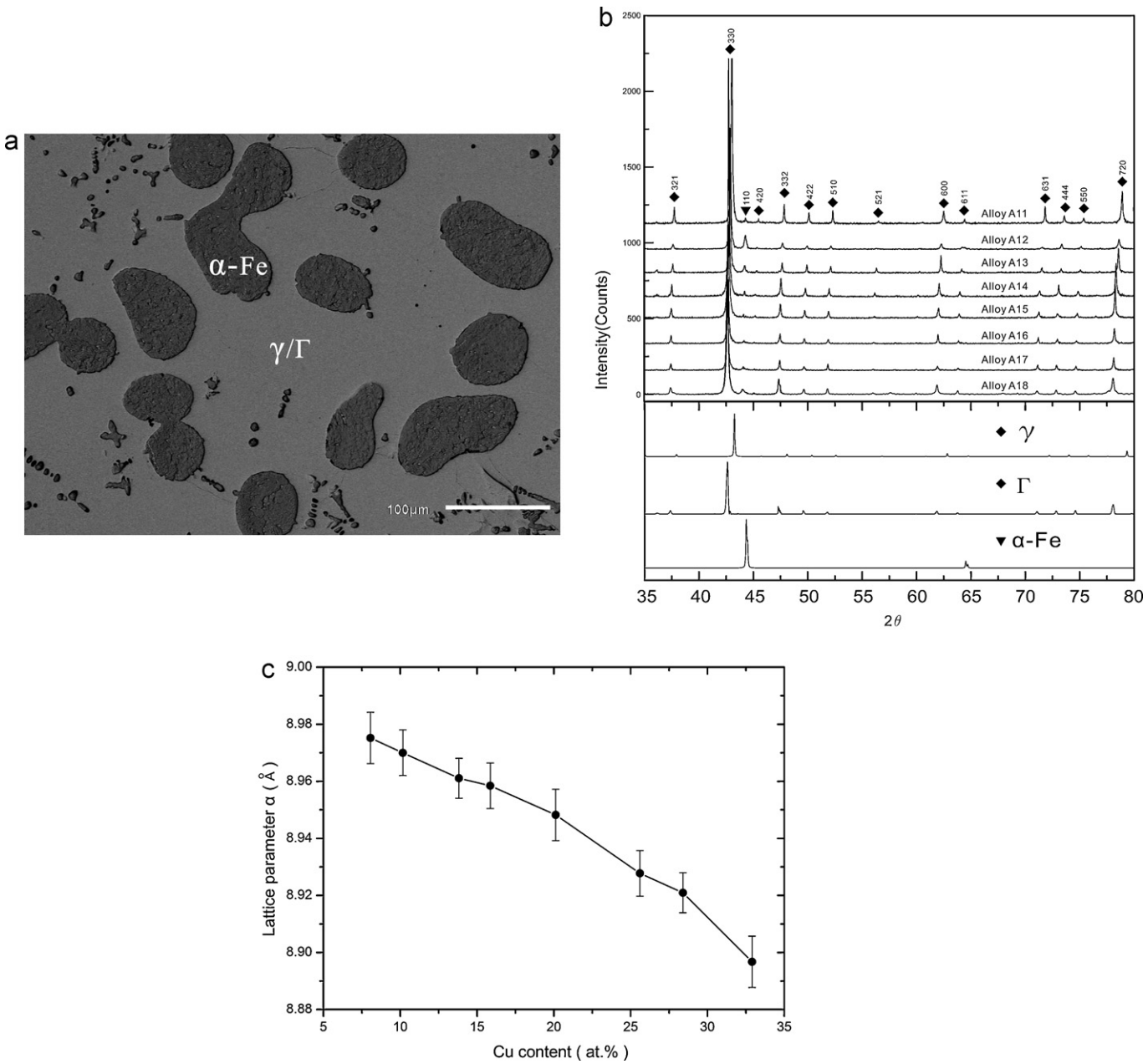

Fig. 4. (a) Two phase, α-Fe and γ/Γ, exist in alloy A11 (Zn_{60}–Fe_{10}–Cu_{30}) at 620 °C. (b) Eight typical X-ray diffraction patterns obtained from the series of alloys (A11–A18) at 620 °C, the peaks of A11 systematically shift to the peaks of A18. Every alloy is composed only of α-Fe and γ/Γ phases. (c) The lattice parameters (α) with standard deviations for the γ/Γ phases containing different amounts of Cu.

(or Γ) in these alloys are marked in Fig. 1 using quadrilateral (♦) and triangular (▲) symbol. The quadrilateral symbol (♦) shows the alloy situates within the γ (or Γ) phase region, it means the specimen is a single phase alloy. Their Zn content is slightly lower than the design composition, which suggests that some Zn was lost in alloy preparation. The triangular symbol (▲) stands on the phase boundary of the γ (or Γ) phase. The composition of γ (or Γ) almost falls on the extension of the line connecting other phase (α-Fe, δ_{Fe} or δ_{Cu}) and the point representing the alloy's composition in the composition triangle. In general, the Zn content in γ (or Γ) is also slightly lower than that calculated using the lever rule. In the γ and Γ phases, the Cu contents decrease gradually from 37.4 at.% to 2.8 at.%, whereas the Fe contents increase from 1.7 at.% to 28.1 at.% (as shown in Fig. 1), this is a consecutive changing process.

Brandon et al. [28] studied the crystal structures of binary phase γ (Cu_5Zn_8) and binary phase Γ (Fe_3Zn_{10}). According to their research, binary phase γ and Γ have the same crystal structure and similar lattice parameter. Eight typical X-ray diffraction patterns obtained from alloy A11–A18 are arrayed in Fig. 4b, every alloy only consists of α-Fe and γ (or Γ). The peaks contributed by α-Fe from these alloys are not obvious, which are found to be shifted to the right with Zn dissolved into α-Fe. Comparing with the binary phase γ, the peaks contributed by the γ phase from alloy A11 shift slightly to lower angles. The peaks (3 3 0) and (6 0 0) existing at diffraction angles $2\theta = 43.297°$ and 62.882° for binary phase γ have shifted to 43.102° and 62.595° for alloy A11, respectively. Calculations indicated that lattice parameter a increases from 8.866 Å for binary phase γ to 8.89673 Å for alloy A11. This suggests that the lattice parameter of the γ phase increases since Fe is dissolved into

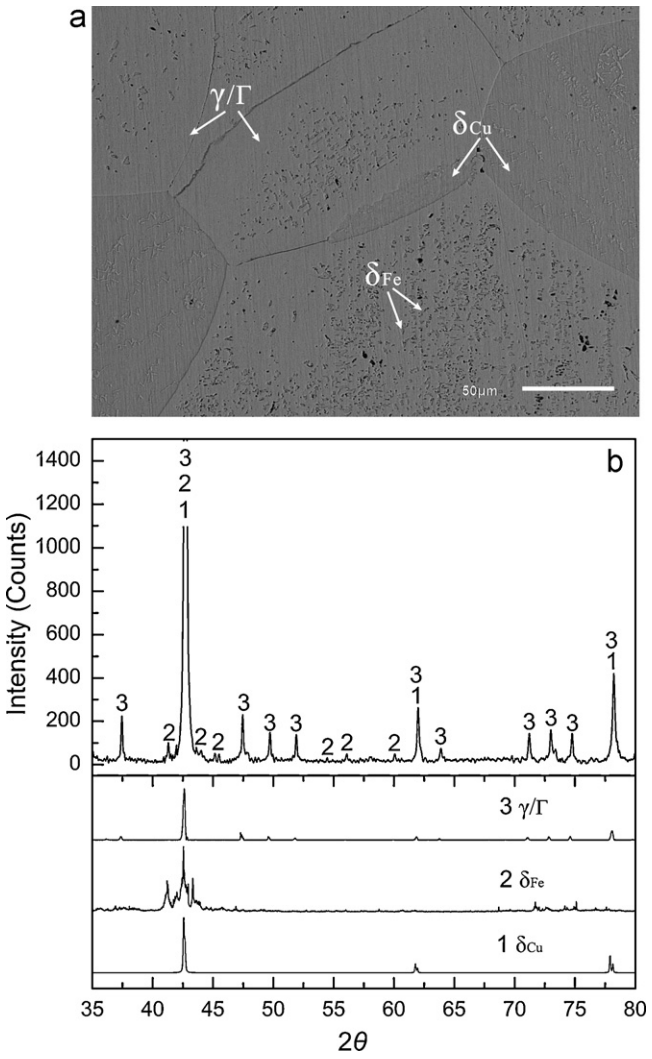

Fig. 5. (a) The BSE micrograph of alloy A5 (Zn_{76}–Fe_6–Cu_{18}) at 620 °C indicates that it consists of three phases: η-Zn, δ_{Fe} and δ_{Cu}. (b) X-ray diffraction pattern of alloy A5 (Zn_{76}–Fe_6–Cu_{18}) shows the coexistence of the three phases γ/Γ, δFe and δCu at 620 °C.

the phase. Alloy A18 was prepared for Γ phase, the X-ray diffraction peaks of Γ phase in alloy A18 have shifted slightly to higher angles. The peaks (3 3 0) and (6 0 0) existing at diffraction angles $2\theta = 42.672^\circ$ and 61.933° for binary phase Γ have shifted to 42.707° and 61.987° for alloy A18, the lattice parameter a has decreased from 8.982 Å to 8.97519 Å compared with the binary phase Γ. The lattice parameters of the Γ phase decreases with increase of Cu content in the phase. As shown in Fig. 4b, the X-ray diffraction peaks contributed by the γ phase (or Γ) shift consecutively from alloy A11 to alloy A18. Fig. 4c plots the graph of the lattice parameters (α, with standard deviations) versus the Cu content in the γ and Γ phases. In a series of the lattice parameters, a linear relationship is displayed for the lattice parameter decreases with the increases of Cu content in the γ and Γ phases. The results obtained from this study indicate that Cu and Fe atoms are mutually interchangeable in the compounds γ and Γ, thereby the γ phase and the Γ phase form a continuous solid solution. The result is agree with the early report by Budurov [9], that the γ and Γ phases form a continuous solid solution at 700 °C. In this work, the continuous solid solution is designated as the γ/Γ phase.

Observed from Fig. 5a, there are three phases, γ/Γ, the δ_{Fe} and δ_{Cu} in alloy A5. Microstructural observations indicated that both γ/Γ and δ_{Fe} exist in the matrix of the δ_{Cu} phase, and the deeply

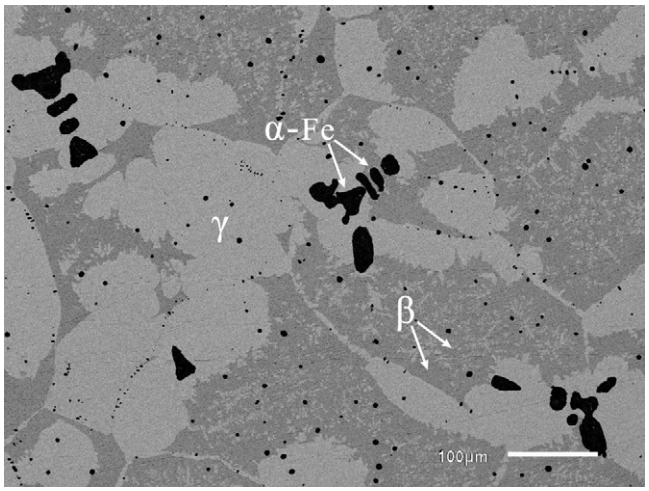

Fig. 6. The BSE micrograph of alloy A19 (Zn_{50}–Fe_{10}–Cu_{40}) at 620 °C indicates that it consists of three phases: α-Fe, γ and β.

etched blocky crystallites are considered as the δ_{Fe} phase, in addition, the compositions of three phases are similar. As shown in Fig. 1, the δ_{Fe} phase and the δ_{Cu} phase extend into the ternary system. The Fe contents of the γ/Γ phase and the δ_{Fe} phase are practically the same 6.5 at.%, however, the γ/Γ phase contains higher Cu than the δ_{Fe} phase. The δ_{Cu} phase contains slightly less Fe and more Cu than the γ/Γ phase. According to Fig. 5b, the peaks contributed by the δ_{Cu} phase and the peaks contributed by γ/Γ phase overlap. Due to the contribution of the δ_{Cu} phase, the intensities of the peaks (6 0 0) and (7 2 1) are higher. There are γ/Γ, δ_{Fe} and δ_{Cu} in alloy A5, which has been confirmed once again by X-ray diffraction analyses.

SEM–WDS and X-ray diffraction analyses confirmed the coexistence of α-Fe, γ and β in alloy A19. The BSE micrograph of alloy A19 is shown in Fig. 6. The γ phase contains 57.5 at.% Zn, 41.7 at.% Cu and only 0.8 at.% Fe. The solubility of Fe in β phases is 0.6 at.%. Alloy A20 is in the (α-Fe + β) two-phase region, and the X-ray diffraction analyses also declared that the two-phase equilibrium state exists in the alloy. The analyses of alloy A21 and A22 confirmed the existence of the three-phase region (α-Fe + β + (Cu)) in 620 °C isothermal sections. The microstructure of alloy A21 is shown in Fig. 7. Three phases, α-Fe, β and (Cu), can be easily differentiated

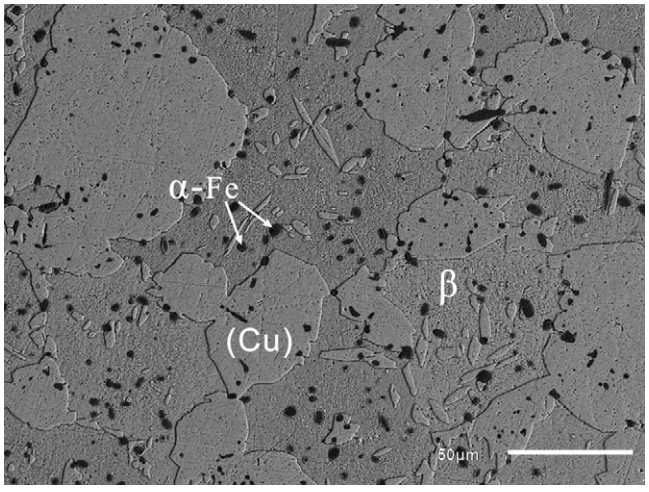

Fig. 7. Three phase: α-Fe, β and (Cu), exist in alloy A21 (Zn_{33}–Fe_{10}–Cu_{57}) at 620 °C.

Table 4
Specimens and phase compositions in the Zn–Fe–Cu ternary system at 800 °C.

Alloy	Designed composition	Phase	Composition (at.%)		
			Zn	Fe	Cu
A2	Zn_{85}–Fe_2–Cu_{13}	η-Zn	84.5	2.1	13.4
A3	Zn_{79}–Fe_2–Cu_{19}	η-Zn	78.4	1.8	19.8
A6	Zn_{80}–Fe_{10}–Cu_{10}	α-Fe	22.7	76.8	0.5
		η-Zn	84.1	4.7	11.2
A7	Zn_{75}–Fe_{10}–Cu_{15}	α-Fe	16.5	82.9	0.6
		η-Zn	80.9	3.4	15.7
A8	Zn_{71}–Fe_{10}–Cu_{19}	α-Fe	13.9	85.4	0.7
		η-Zn	79.8	2.9	17.3
		γ	69.8	3.6	26.6
A10	Zn_{66}–Fe_2–Cu_{32}	γ	65.2	2.2	32.6
A11	Zn_{60}–Fe_{10}–Cu_{30}	α-Fe	10.5	88.8	0.7
		γ	63.5	2.9	23.6
A12	Zn_{62}–Fe_{10}–Cu_{28}	α-Fe	11.9	87.5	0.6
		γ	66.2	3.1	30.7
A19	Zn_{50}–Fe_{10}–Cu_{40}	α-Fe	6.8	92.4	0.8
		γ	55.5	2.6	41.9
		β	48.2	1.4	50.4
A20	Zn_{40}–Fe_{10}–Cu_{50}	α-Fe	3.7	95.4	0.9
		β	43.1	1.5	55.4
A21	Zn33–Fe10–Cu57	α-Fe	1.5	97.4	1.1
		β	37.6	1.9	60.5
		(Cu)	31.9	1.3	66.8
A22	Zn20–Fe10–Cu70	α-Fe	0.9	98.0	1.1
		(Cu)	21.9	1.2	76.9

from its morphology and chemical compositions. SEM–WDS analyses indicated that the apex of the α-Fe + β + (Cu) phases triangle at the (Cu) phase boundary is approximately 34.7 at.% Zn and 0.6 at.% Fe at 620 °C. The identities of the phases in alloy A21 have been confirmed by X-ray diffraction analyses.

4.2. The 800 °C isothermal section of the Zn–Fe–Cu ternary system

Twelve alloys were prepared for studying the 800 °C isothermal section of the Zn–Fe–Cu ternary system. The specimens and phase compositions are shown in Table 4. Alloy A2 and A3 were annealed at 800 °C and examined again, the results indicated that they locate in the η-Zn single-phase region, and their Fe contents in η-Zn phase are 2.1 at.% and 1.8 at.%, respectively.

The alloy A6–A12 were annealed for 15 days, then SEM–WDS and X-ray diffraction analyses revealed that the phase relationships of the α-Fe phase, the η-Zn phase and the γ phases. The α-Fe phase coexists with the η-Zn phase in Alloy A6 and alloy A7. The Fe solubility of the η-Zn phase in alloy A6 and A7 is 4.7 at.% and 3.4 at.%, respectively. The solubility increases with the increase of the temperature and the decrease of Cu content in the η-Zn phase. The maxima solubility is 8.4 at.%, which lies on the Zn-Fe axis. SEM–WDS and X-ray diffraction analyses revealed the alloy A8-A9 consists of α-Fe, η-Zn and γ. The γ phase contains 69.8 at.% Zn, 3.6 at.% Fe and 26.6 at.% Cu in alloy A8. It extends to the Zn–Fe-rich side in the 800 °C isothermal section. Based on the formation of the γ/Γ continuous solid solution with at 620 °C, this trend was reasonable. The γ single-phase alloy A10 and the two-phase alloy A11 and A12 (α-Fe + γ) also confirms the extension of γ phase boundary.

The phase relationships in alloy A19 and A20 at the 800 °C isothermal sections are in full agreement with that at the 620 °C isothermal sections. The BSE micrograph of alloy A19 at 800 °C is shown in Fig. 8. It confirms the coexistence of α-Fe, γ and β in alloy A19. The sample was deeply etched using aqueous solution mixed ferric chloride and hydrochloride. Because of its low relief, the γ phase is easy to identify compared with the one in Fig. 6. The γ phase at 800 °C contains 55.5 at.% Zn, 41.9 at.% Cu and 2.6 at.% Fe, it contains more Fe than that at 620 °C. The solubility of Fe in

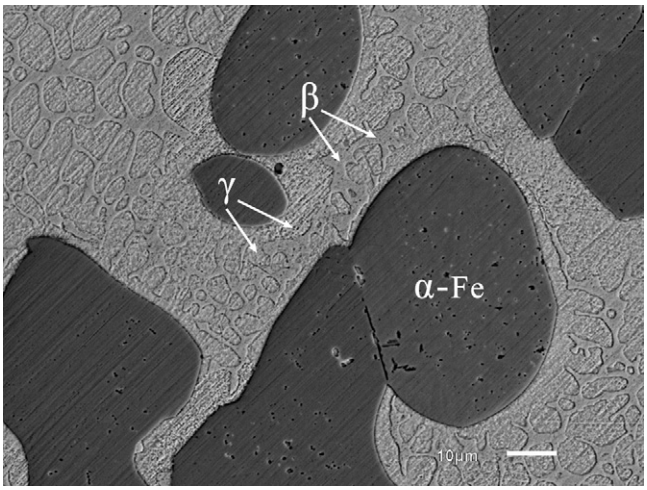

Fig. 8. The BSE micrograph of alloy A19 (Zn_{50}–Fe_{10}–Cu_{40}) at 800 °C indicates that it consists of three phases: α-Fe, γ and β.

β phases at 800 °C is also higher than that at 620 °C, it increases from 0.6 at.% to 1.4 at.%. SEM–WDS and X-ray diffraction analyses declared that alloy A20 locates in the (α-Fe + β) two-phase region at 800 °C. The analyses of alloy A21 and A22 also confirmed the (α-Fe + β + (Cu)) three-phase region exists in the 800 °C isothermal section. The microstructure of alloy A21 at 800 °C is ultrafine difference compared with that at 620 °C. But the (Cu) phase contains 31.9 at.% Zn, 1.3 at.% Fe and 66.8 at.% Cu at 800 °C, the solubility of Fe in (Cu) phases is higher than that at 620 °C. Alloy A22 stands within the (α-Fe + (Cu)) two-phase region, and its X-ray diffraction analyses also confirmed that the two-phase equilibrium state exists in the alloy.

5. Conclusion

Based on the SEM–WDS and X-ray diffraction analyses of ternary alloys, the phase relationships of the Zn–Fe–Cu system at 620 °C and 800 °C were determined in this study. The following findings can be concluded from this work:

1. Four three-phase regions have been identified in the Zn–Fe–Cu ternary system at 620 °C, and three three-phase regions have been confirmed in the Zn–Fe–Cu ternary system at 800 °C. The α-Fe phase coexists with the γ phase and the β phase at 620 °C and 800 °C.
2. The Fe solubility in η-Zn increases with the increase of the temperature and the decrease of Cu content in η-Zn phase, the maxima solubility is 8.4 at.% at 800 °C. The solubility of Fe in β and (Cu) at 800 °C is about 1.9 at.% and 1.3 at.%, respectively. Corresponding solubility at 620 °C are lower than that at 800 °C.
3. The γ and Γ phases form a continuous solid solution at 620 °C, which was designated as the γ/Γ phase. The lattice parameters of the γ/Γ phase increases with increase of Fe in the γ/Γ phase. The α-Fe phase and the γ/Γ phase form a two-phase region.
4. Binary phase δ_{Fe} and δ_{Cu} extend into the ternary system at 620 °C. The phase coexistent relationship of the γ/Γ, δ_{Fe} and δ_{Cu} has been confirmed, their compositions are very similar, the three-phase triangle of ($\gamma/\Gamma + \delta_{Fe} + \delta_{Cu}$) was small and narrow.
5. Binary phase γ extends to the Zn–Fe-rich side at 800 °C. The lowest Cu content is about 27.6 at.% and the highest Fe content reaches to 3.6 at.% in the γ phase.

Acknowledgements

This investigation is supported by National Natural Science Foundation of China (Nos. 50971110 and 50971111), Qinlan project and Hunan Provincial Innovation Foundation for Postgraduate (No. CX2010B261).

References

[1] A. Marder, Prog. Mater. Sci. 45 (2000) 191–271.
[2] J. Selverian, A. Marder, M. Notis, Metall. Mater. Trans. A 20 (1989) 543–555.
[3] J. Selverian, A. Marder, M. Notis, Metall. Mater. Trans. A 19 (1988) 1193–1203.
[4] T. Ooi, Y. Sugimoto, S. Fujita, GALVATECH'07 (2007) 562–567.
[5] N. Katiforis, G. Papadimitriou, Surf. Coat. Technol. 78 (1996) 185–195.
[6] D. Gittings, D. Rowland, J. Mack, Trans. ASM 43 (1951) 587–610.
[7] J. Miettinen, Calphad 32 (2008) 514–519.
[8] M. Avettand-Fènoël, A. Hadadi, G. Reumont, P. Perrot, J. Mater. Sci. 43 (2008) 1740–1744.
[9] S. Budurov, Izv. Po. Khimiya Sofia 11 (1978) 517–559.
[10] X. Su, N.-Y. Tang, J.M. Toguri, J. Alloys Compd. 325 (2001) 129–136.
[11] J. Nakano, D.V. Malakhov, G.R. Purdy, Calphad 29 (2005) 276–288.
[12] W. Xiong, Y. Kong, Y. Du, Z.-K. Liu, M. Selleby, W.-H. Sun, Calphad 33 (2009) 433–440.
[13] G. Reumont, P. Perrot, J. Fiorani, J. Hertz, J. Phase Equilib. Diffus. 21 (2000) 371–378.
[14] P. Spencer, Calphad 10 (1986) 175–185.
[15] M. Kowalski, P. Spencer, J. Phase Equilib. 14 (1993) 432–438.
[16] W. Gierlotka, J. Mater. Res. 23 (2008) 258–263.
[17] O. Kubaschewski, J. Smith, D. Bailey, Z. Metallkd. 68 (1977) 495–499.
[18] P.A. Lindqvist, B. Uhrenius, Calphad 4 (1980) 193–200.
[19] M. Hasebe, T. Nishizawa, Calphad 5 (1981) 105–108.
[20] Y.Y. Chuang, R. Schmid, Y.A. Chang, Metall. Mater. Trans. A 15 (1984) 1921–1930.
[21] Q. Chen, Z. Jin, Metall. Mater. Trans. A 26 (1995) 417–426.
[22] D. Cook, R. Grant, Identification of the Iron–Zinc Phases in Galvanneal Steel Coatings by Mossbauer Spectroscopy and X-ray Diffraction. Phase I. Characterization of the Fe–Zn Intermetallic Phases, International Lead Zinc Research Organization Report, 1993.
[23] S. Shimizu, Y. Murakami, S. Kachi, J. Phys. Soc. Jpn. 41 (1976) 79.
[24] E. Owen, L. Pickup, Proc. R. Soc., Lond. Ser. A 140 (1933) 179–191 (Containing Papers of a Mathematical and Physical Character).
[25] O. Gourdon, D. Gout, D. Williams, T. Proffen, S. Hobbs, G. Miller, Inorg. Chem. 46 (2007) 251–260.
[26] J. Lenz, K. Schubert, Z. Metallkd. 62 (1971) 810–816.
[27] X.P. Su, N.-Y. Tang, J.M. Toguri, Can. Metall. Q. 40 (2001) 377–384.
[28] J.K. Brandon, R.Y. Brizard, P.C. Chieh, R.K. McMillan, W.B. Pearson, Acta Crystallogr. B 30 (1974) 1412–1417.